



6<sup>th</sup> International Symposium on Space Sailing (ISSS 2023), New York, USA, 5-9 June 2023

# Long-term mission of the spacecraft with a degrading solar sail into the asteroid belt

Bakhyt N. ALIPOVA<sup>a,\*\*</sup>, Olga L. STARINOVA<sup>b</sup>, Miroslav A. Rozhkov<sup>b</sup>

<sup>a</sup>*Department of Aerospace and Mechanical Engineering, University of Kentucky, Lexington KY, USA,  
International Information Technology University, Almaty, Kazakhstan*

<sup>b</sup>*Flight Dynamics and Control Theory Department, Samara national Research University, Samara, Russia*

---

# Our Team



**Olga Starinova**



**Miroslav Rozhkov**

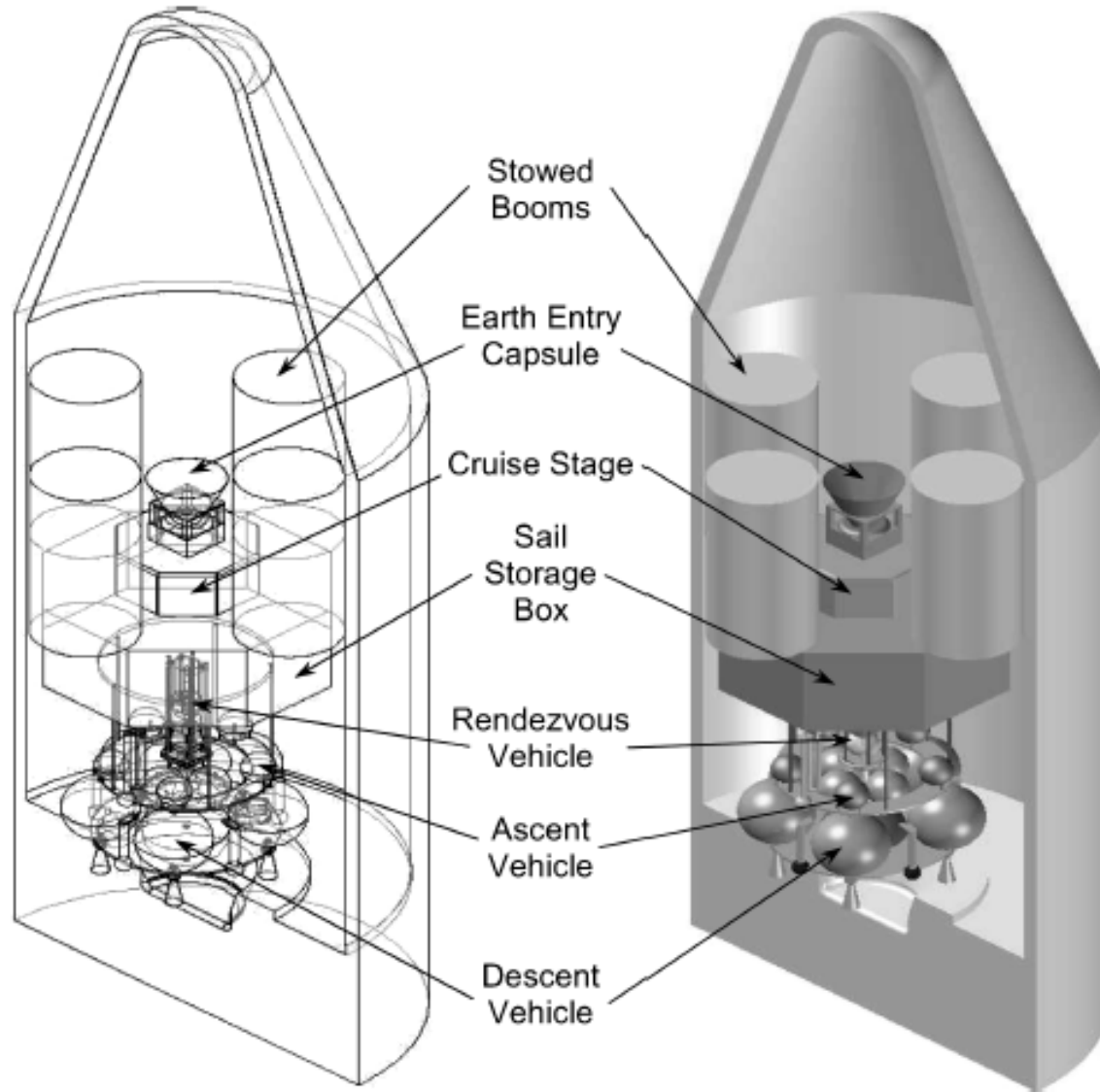
**Flight Dynamics and Control Theory Department,  
Samara National Research University, Samara, Russia**

# **Description of the ballistic scheme of the mission and the design parameters of the spacecraft**

## **Ballistic scheme of the mission**

- A spacecraft with a folded sail is brought out of the Earth's sphere of action onto a heliocentric flight trajectory that provides the specified parameters of a gravitational maneuver near the Earth due to the propulsion system of the upper stage.
- A year later, after performing a gravitational maneuver in the Earth's gravity field, the spacecraft fairing is reset and the solar sail opens.
- Further heliocentric movement is carried out due to light pressure and the spacecraft enters orbit, most of the time lying in the asteroid belt.
- The solar sail assumes a position perpendicular to the light stream, and further trajectory changes occur only due to the degradation of the sail surface, long-term studies of the asteroid belt are carried out.

# Prototype spacecraft and sails



As a prototype, the solar sail of the SPACECRAFT project is used to deliver soil samples from the surface of Mercury to Earth. According to the calculations, a frame-type solar sail delivered by a Japanese H-2A launch vehicle with an excess of speed to reach a heliocentric trajectory will be able to give a payload weighing 1905 kg an acceleration of  $0.25 * 10^{-3} \text{ m/s}^2$ .

**Figure:** Placement of a spacecraft with a solar sail delivering soil from the surface of Mercury under the fairing of the H-IIA launch vehicle

From: G.W. Hughes, M. Macdonald, C.R. McInnes et al. Sample Return from Mercury and Other Terrestrial Planets Using Solar Sail Propulsion, *Journal of Spacecraft and Rockets*, 43 (2006).

**Table 1 – Design parameters of the spacecraft**

Weight of the spacecraft, kg	Payload weight, kg	The mass of the solar sail, kg	Sail shape, m	Acceleration, mm/s <sup>2</sup>
2353	1905	448	275x275	0.25

**Table 2 – Mass characteristics of the solar sail for the delivery of Mercury soil**

Element Description	Weight, kg
Payload weight of the sail	1905
The bearing film of the CP1 sail is 2 mkm	216
Aluminum reflective coating with a thickness of 0.1 mkm	41
Binding coating	26
Frame beams sails	54
Mechanical deployment and management systems	111
Total mass of solar sail assembly	448
Initial mass of the spacecraft	2353

Dimensions of the solar sail: 275m x 275m

Sail area: 75'625 m<sup>2</sup>

Characteristic acceleration: 0.25 mm/s<sup>2</sup> (Earth to Mercury),  
0.78 mm/s<sup>2</sup> (return)

Energy characteristics of the Japanese H-IIA 202-4S launch vehicle with the reference of which the device was designed, make it possible to put up to 2,600 kg of payload into a parabolic orbit out of the Earth's sphere of action (11.2 km/s).

# Lighter Spacecraft Option (for research purposes)

- Choice a lighter spacecraft weighing 500 kg (for research purposes)
- Sail area reduced to 16'070 m<sup>2</sup>

Table 3 – Parameters of the selected spacecraft

Design parameters of the device		
Initial mass of the spacecraft, kg		500
Sail area, m <sup>2</sup>		16070
Reflection Coefficient (Al)		0,777
Specular Reflection Factor (Al)		0,900
Secondary radiation coefficient	Al	0,540
	Cr	0,540
Non-Lambert coefficient	Al	0,790
	Cr	0,550



**The mathematical model used for the  
motion of a spacecraft  
with a solar sail**



The following assumptions are used to describe the motion of the spacecraft:

- the motion of the spacecraft in the plane of the ecliptic is considered, the orbits of the planets are considered circular;

- gravitational or other disturbances from any celestial objects are not taken into account;

- the intensity of the Sun's radiation varies inversely proportional to the square of the distance and does not change with time (does not depend on solar activity).

$$\frac{dr}{dt} = V_r, \quad \frac{dV_r}{dt} = a_r(r, \lambda_1, t) - \frac{1}{r^2} + \frac{V_u^2}{r},$$

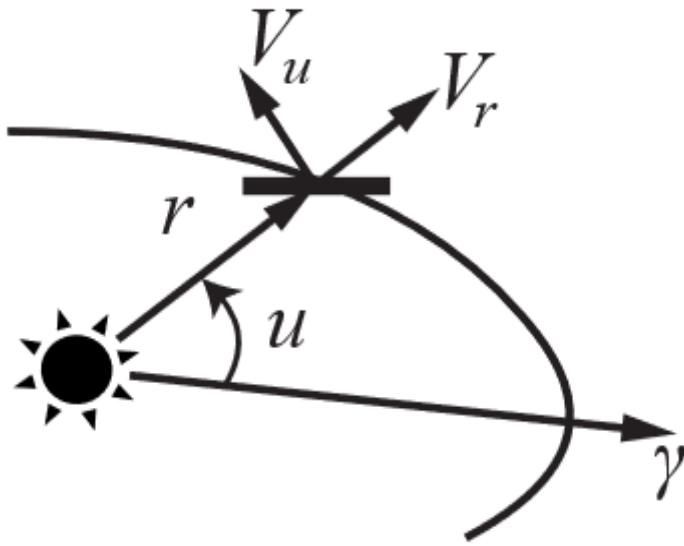
$$\frac{du}{dt} = \frac{V_u}{r}, \quad \frac{dV_u}{dt} = a_u(r, \lambda_1, t) - \frac{V_r V_u}{r}$$

Describes motion in a flat polar coordinate system

Dimensionless form

Equations describe the motion:

- Differential equations for radius and velocity components
- Acceleration generated by the solar sail depends on distance and angle of the sail



### Coordinates and directions of vector

- Coordinates:  $r$  (radius vector) and  $u$  (latitude argument)
- Velocity components:  $V_r$  (radial) and  $V_u$  (transversal)
- Acceleration components:  $a_r$  and  $a_u$

**Fig. 2.** Polar plane heliocentric coordinate system

## Boundary Conditions

$$t = T, \quad r = r_t, \quad V_r = V_{r_t}, \quad V_u = V_{u_t},$$

Boundary conditions for achieving the spacecraft's target orbit

Duration of flight:  $T$

Heliocentric radius and velocity components in the target orbit:  $r_t, V_{r_t}, V_{u_t}$

Depend on the angle of the true anomaly at the final moment of time

# Components of Acceleration

Sum of two components: directed along the normal to the surface of the sail ( $a_{\perp}$ ) and parallel to the surface of the sail in a plane passing through the radius vector ( $a_{\parallel}$ )

Equations (1) and (2) describe the components of acceleration

$$a_{\perp} = \frac{S_r}{cm} S \cdot \cos \theta \cdot (a_1 \cos \theta + a_2) \quad (1)$$

$$a_{\parallel} = \frac{S_r}{cm} S \cdot \cos \theta \cdot a_3 \sin \theta \quad (2)$$

$$a_1 = 1 + \zeta \rho,$$

$$a_2 = B_f (1 - \zeta) \rho + (1 - \rho) \frac{\varepsilon_f B_f - \varepsilon_b B_b}{\varepsilon_f + \varepsilon_b},$$

$$a_3 = 1 - \zeta \rho$$

where  $S_r$  - is the power of the solar electromagnetic wave incident on a unit surface of a sail located at a heliocentric distance  $r$ ;

$c$  - the speed of light;

$m$  - the mass of the spacecraft;

$S$  - surface area of the sail;

$\theta$  - the angle between the direction to the Sun and the normal to the surface of the sail (installation angle);

$\rho$  - reflection coefficient;  $\zeta$  - the mirror reflection factor of the sail surface;  $\varepsilon_f, \varepsilon_b$  - the radiation coefficients of the front and rear surfaces of the sail;

$B_f, B_b$  - are non-Lambert coefficients of the front and rear surfaces of the sail, which describe the angular distribution of emitted and diffusely reflected photons.

The power of the solar electromagnetic wave varies inversely-proportional to the square of the heliocentric distance:

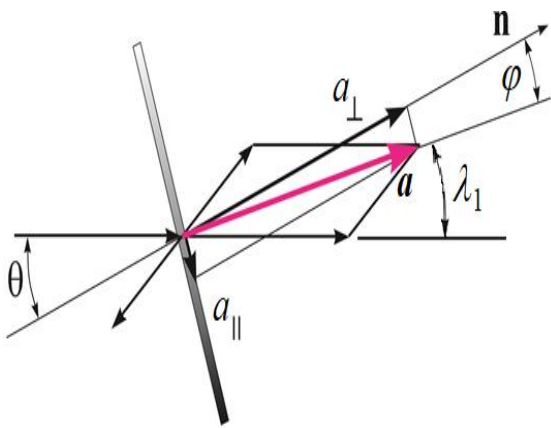
$$S_r = S_0 \left( \frac{r_0}{r} \right)^2, \quad (6)$$

where  $S_0 = 1,36 \cdot 10^3 \text{W/m}^2$  – solar constant (the intensity of the Sun's radiation in the Earth's orbit),

$r_0 = 1\text{AU} = 1,496 \cdot 10^8 \text{ km}$  - is the average distance from the Earth to the Sun.

## Thrust

- Equations (3) and (4) describe the thrust from light pressure and the deviation of thrust direction from the sail surface's normal
- Impact of imperfect reflection on thrust magnitude and direction



$$a = \frac{S_r}{cm} S \cos \theta \sqrt{1 + 2\zeta\rho \cos 2\theta + (\zeta\rho)^2 + 2a_2(1 + \zeta\rho) \cos \theta + a_2^2} \quad (3)$$

$$tg \varphi = \frac{a_{||}}{a_{\perp}} = \frac{a_3 \sin \theta}{a_1 \cos \theta + a_2} = \frac{(1 - \zeta\rho) \sin \theta}{(1 + \zeta\rho) \cos \theta + a_2} \quad (4)$$

$$a = \frac{S_r}{cm} S(\theta) \sqrt{1 + \rho^2 - 2\rho \cos(\pi - 2\theta)} = \frac{S_r}{cm} S \cos \theta \sqrt{1 + \rho^2 + 2\rho \cos 2\theta}, \quad (5)$$

$$\sin \varphi = \frac{(1 - \rho) \sin \theta}{\sqrt{1 + \rho^2 + 2\rho \cos 2\theta}}. \quad (6)$$

### Conclusions:

- (1) a decrease in the magnitude of acceleration from the forces of light pressure
- (2) a narrowing of the range of available acceleration angles relative to the direction of the luminous flux
- (3) an increase in the share of absorbed energy of the luminous flux, which leads to an increase in surface temperature and acceleration of degradation processes of the sail surface.

## Degradation of Soil surface optical parameters

Surface degradation due to outer space factors [Dachwald, McDonald, McInnes et al]:  
Decrease in reflection coefficient, increase in absorbed radiation.

Parametric dependencies for calculating changes in optical characteristics

$$\frac{p(t)}{p_0} = \begin{cases} \frac{1+de^{-\lambda\Sigma(t)}}{1+d} & \text{for } p \in \{\rho, \varsigma\}, \\ 1 + d(1 - e^{-\lambda\Sigma(t)}) & \text{for } p = \varepsilon_f, \\ 1 & \text{for } p \in \{\varepsilon_b, B_f, B_b\}, \end{cases} \quad (7)$$

Total dose of solar radiation received during the flight

$$\Sigma(t) = \frac{\tilde{\Sigma}(t)}{\tilde{\Sigma}_0} = \frac{r_0^2}{T_0} \int_{t_0}^t \frac{\cos \theta(t)}{r(t)^2} dt \quad (8)$$

where  $T_0 = 365 \cdot 24 \cdot 3600$  s – corresponds to one year in seconds.

where  $\Sigma(t)$  – the dimensionless total dose of solar radiation received during the flight;  
 $\lambda$  - degradation coefficient;  $d$  - degradation factor.

The dimensionless total dose of solar radiation is calculated as the ratio of the total radiation power received by the sail during the flight to the solar radiation power received by a platform of 1  $m^2$  at a distance of 1 AU, for one year  $\tilde{\Sigma}_0 = 15,768 \cdot 10^{12}$  J/ $m^2$ .

## Degradation Coefficient

The degradation coefficient  $\lambda$  is determined based on half the lifetime of the sail under the influence of solar radiation:

$$\lambda = \frac{\ln 2}{\hat{\Sigma}}. \quad (13)$$

where  $\hat{\Sigma}$  - the dose of solar radiation, which leads to a half deterioration of optical characteristics, that is, corresponds to the value of the optical characteristic.

$$\hat{p} = \frac{p_0 + p_\infty}{2}.$$



## Degradation Factor

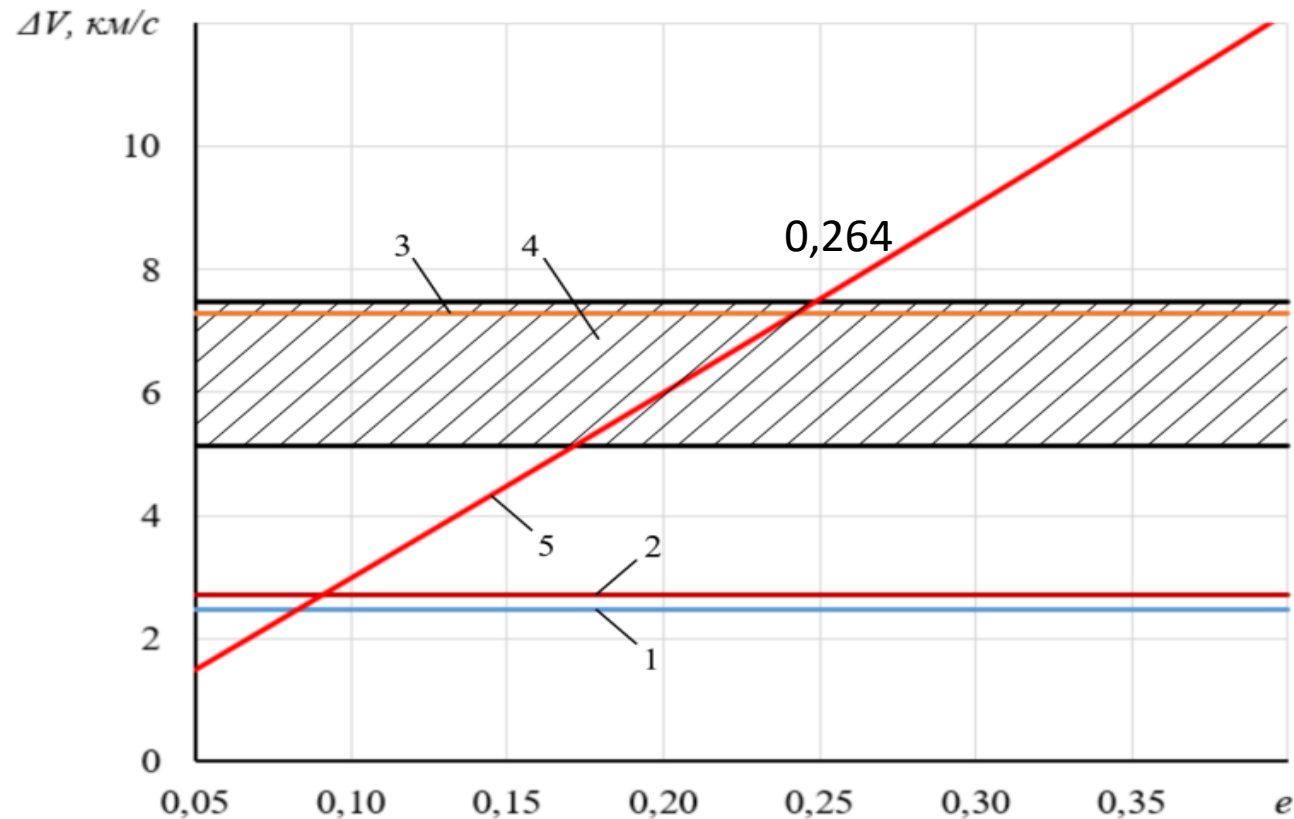
The degradation factor  $d$  determines the value of the optical characteristic  $p_\infty$ , at which the sail should stop functioning. At the same time

$$\rho_\infty = \frac{\rho_0}{1+d}, \quad \zeta_\infty = \frac{\zeta_0}{1+d}, \quad \varepsilon_{f\infty} = \varepsilon_{f0}(1+d) \quad (14)$$

Even a preliminary analysis of formulas at Eq.11. – 14. shows that the acceleration from the solar sail, and, consequently, the laws of sail control and the corresponding trajectories of motion depend on the optical characteristics of the surface, and the optical characteristics, in turn, depend on the laws of control and flight path. Therefore, a comprehensive analysis of possible interplanetary missions of spacecraft with a solar sail requires taking into account all these interrelated parameters.

## *Mission Assumptions:*

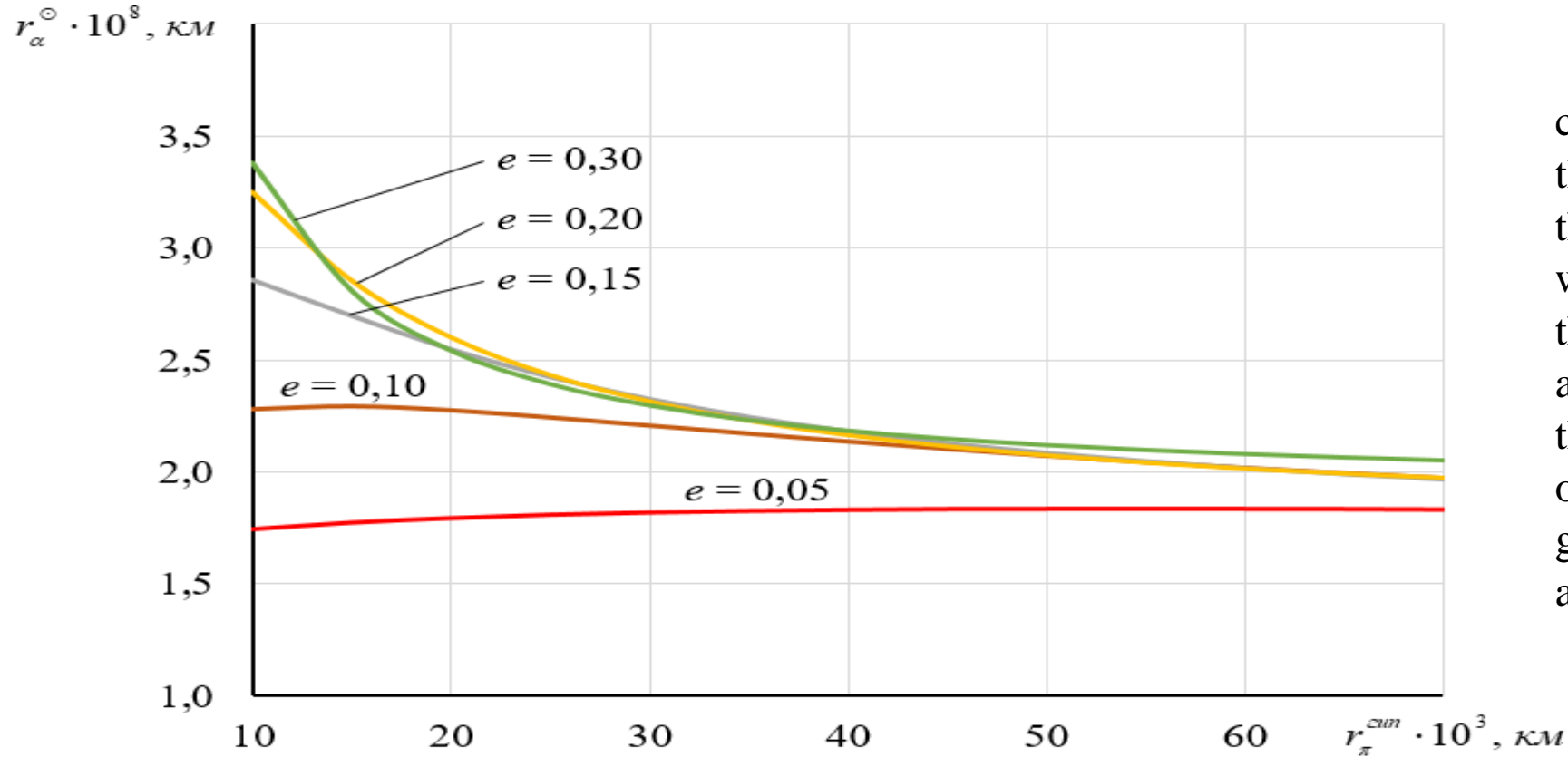
- Trajectory lies in the plane of the ecliptic.
- Earth's orbit is circular.
- Passive motion of the spacecraft after leaving Earth's sphere of action in an orbit with a large semi-axis of 1 AU.
- Next meeting with Earth occurs in a year.
- Variable parameters: eccentricity of Earth-to-Earth flight orbit and radius of pericentre of geocentric hyperbola during gravitational manoeuvre.



Dependence of the required velocity on the eccentricity of the transition orbit.

- 1 – Venus,
- 2 – Mars,
- 3 – Mercury,
- 4 – Asteroid belt,
- 5 – characteristic speed to create an Earth-Earth orbit with a given eccentricity

# Aphelion of Resulting Orbit



We will use in further calculations a safe distance from the center of the Earth of 10 thousand km and we will get that with the selected eccentricity of the orbit, the maximum value of aphelion 2.27 AU is achieved with the eccentricity of the heliocentric orbit after performing a gravitational manoeuvre 0.41506 and a large semi-axis 1.70958 AU.

Aphelion of Resulting Orbit vs. Geocentric Perigee and Eccentricity of Transition shows aphelion radii of passive orbits achievable after gravitational manoeuvre.

- Higher aphelion achieved at smaller radii of geocentric pericenter for eccentricities  $> 0.15$ .
- Selected eccentricity of the orbit yields maximum aphelion of 2.27 AU.

# Heliocentric Motion Control after Gravity Manoeuvre

- Equations of motion and acceleration projections: Solar sail acceleration ( $a$ ) has two projections: radial and transversal.
- Equations (9) and (10) provide the scalar values of the projections.

$$a_r = a_{\perp} \cos \theta + a_{\parallel} |\sin \theta| = a_{\perp} \cos(\lambda_1 + \varphi) + a_{\parallel} |\sin(\lambda_1 + \varphi)|, \quad (9)$$

$$a_u = a_{\perp} \sin \theta - a_{\parallel} \cos \theta \cdot \text{sign}(\theta) = a_{\perp} \sin(\lambda_1 + \varphi) - a_{\parallel} \cos(\lambda_1 + \varphi) \cdot \text{sign}(\lambda_1 + \varphi) \quad (10)$$

We will look for the law of changing the angle of the sail  $\lambda_1 \in \left[-\frac{\pi}{2}; \frac{\pi}{2}\right]$ , such that it reaches the required orbit as soon as possible, that is, the boundary conditions in Eq. 2 are met and the minimum functionality is provided by

$$T = \int_0^T dt \rightarrow \min. \quad (11)$$

## Hamiltonian Formulation:

- Hamiltonian equation (12) derived from the system of equations.

$P_r, P_u, P_{V_r}, P_{V_u}$  – conjugate variables,  $a_c$  – nominal maximum acceleration acting on the sail at a distance of 1 AU.

### Control Law and Maximum Hamiltonian:

- According to the Pontryagin maximum principle, control law maximizing the Hamiltonian is known.
- Equation (13) defines  $\lambda_1$  based on conjugate variables also eta is calculated based on conjugate variables

$$H = P_r \cdot V_r + P_u \cdot \frac{V_u}{r} + P_{V_r} \left( \frac{V_u^2}{r} - \frac{1}{r^2} + \frac{a_c}{r^2} \cos^3 \lambda_1 \right) + P_{V_u} \left( -\frac{V_u V_r}{r} + \frac{a_c}{r^2} \cos^2 \lambda_1 \sin \lambda_1 \right)$$

$$H = V_r \psi_r + \frac{V_u}{r} \psi_u + \left( a_c \frac{\cos^3 \theta}{r^2} - \frac{1}{r^2} + \frac{V_u^2}{r} \right) \psi_{V_r} + \left( a_c \frac{\cos^2 \theta \sin \theta}{r^2} - \frac{V_u V_r}{r} \right) \psi_{V_u}, \quad (12)$$

$$\lambda_1 = \frac{1}{2} \left( \eta - \arcsin \frac{P_{V_u}}{3 \sqrt{P_{V_r}^2 + P_{V_u}^2}} \right),$$

(13)

where  $\eta = \arccos \frac{P_{V_r}}{\sqrt{P_{V_r}^2 + P_{V_u}^2}}$ .

- Two-Point Boundary Value Problem:

Optimal control and trajectory determined by solving a two-point boundary value problem.

The system of equations is supplemented by differential equations (equation set given below) for conjugate variables.

⇒

- Optimal Control with Varying Angular Range:

If the angular range of the flight is not fixed, finding optimal control becomes a three-parameter boundary value problem.

Initial values of conjugate variables are determined to satisfy boundary conditions.

$$\frac{dP_r}{dt} = P_{V_r} \left( \frac{V_u^2}{r^2} - \frac{2}{r^3} \right) - P_{V_u} \frac{V_r V_u}{r^2} + \frac{2a_c}{r^3} \cos^3 \lambda_1,$$

$$\frac{dP_u}{dt} = 0 \Rightarrow P_u \equiv \text{const},$$

$$\frac{dP_{V_r}}{dt} = -P_r + P_{V_u} \frac{V_u}{r},$$

$$\frac{dP_{V_u}}{dt} = \frac{P_{V_u} V_r - 2P_{V_r} V_u}{r}.$$

# The results obtained during the simulation

Energy capabilities allow launch of spacecraft with eccentricity of 0.264.

Table 4: Parameters of spacecraft's heliocentric orbit before and after gravitational manoeuvre.

	Intermediate orbit Earth-Earth	Orbit after gravitational manoeuvre
Big half-axis, million km	149.6	255.75273
Eccentricity	0.264	0.41506
The angle of the true anomaly, deg	105.308	37.233
Radial component of the spacecraft velocity, km/s	7.863	4.802
Transversal component of the spacecraft velocity, km/s	28.728	34.631

# Solar sail unfolds after gravitational manoeuvre

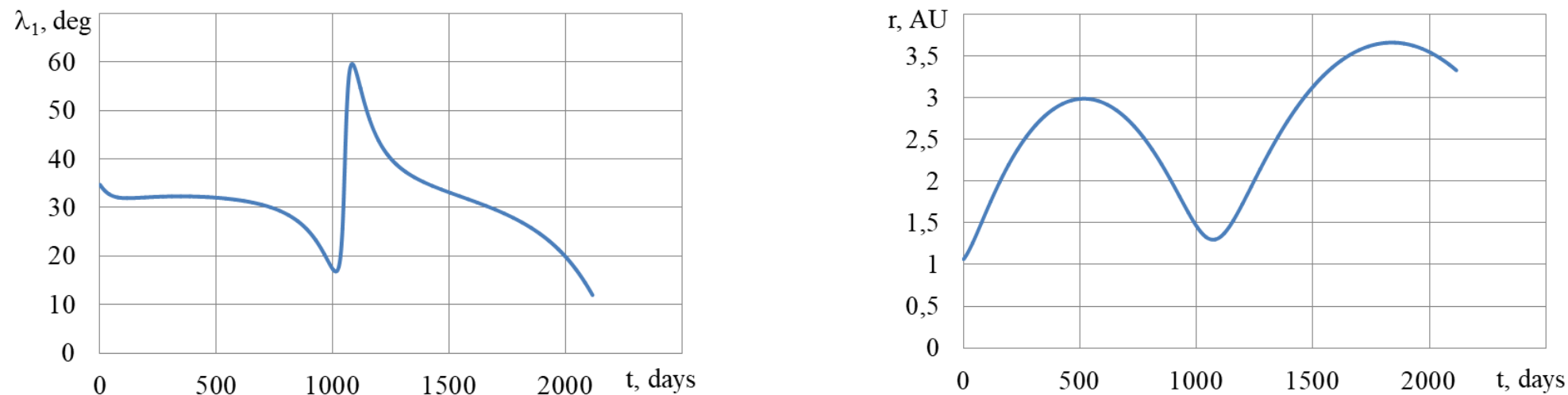


Figure 1: Optimal change in sail angle and spacecraft's radius vector.

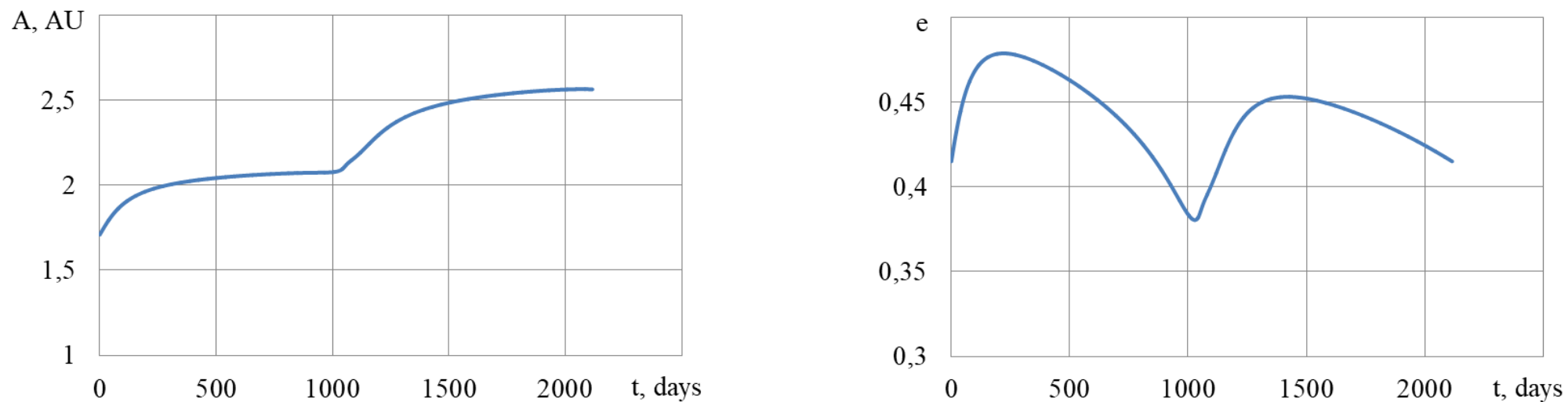
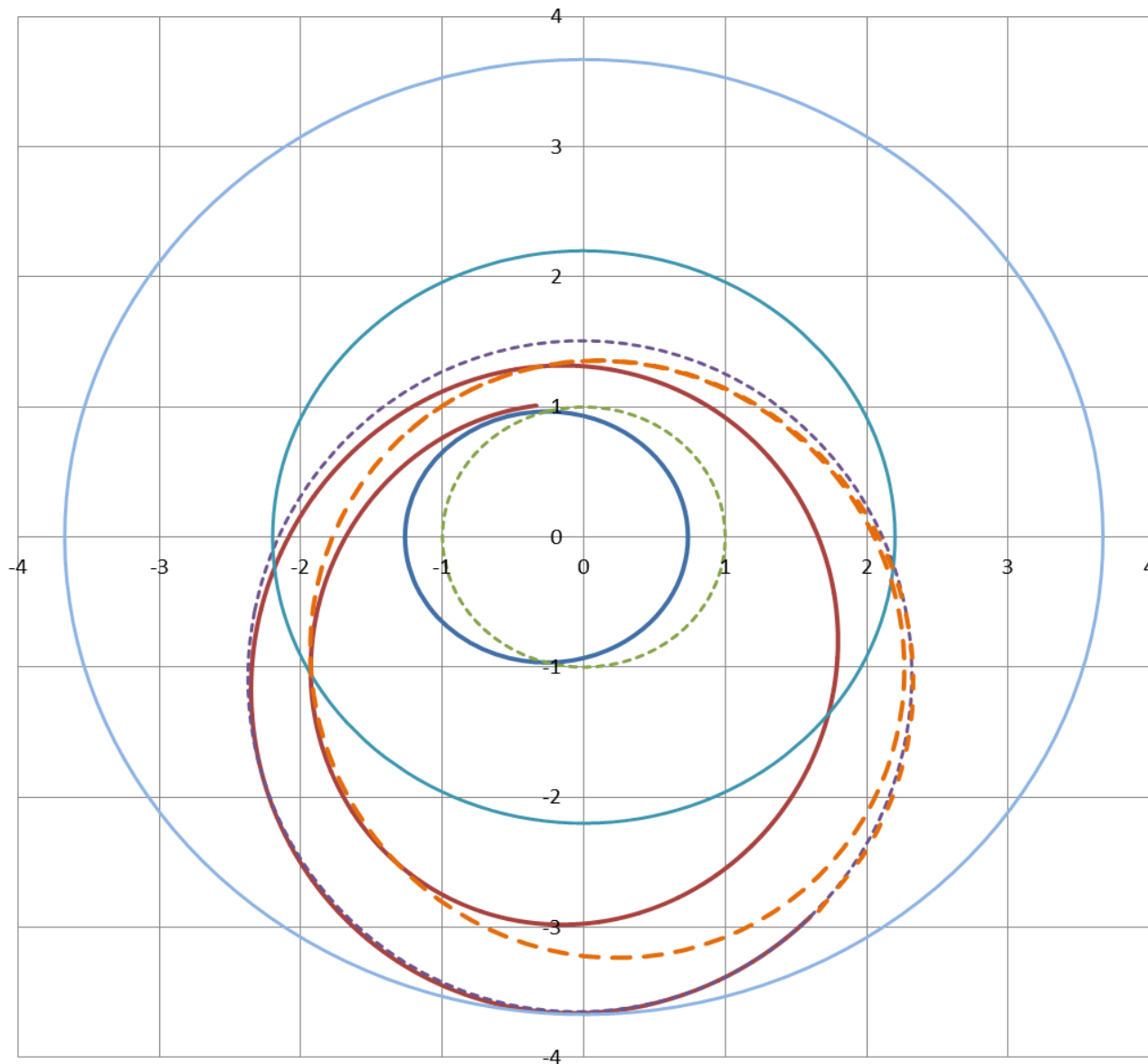


Figure 2: Change in the semimajor axis and eccentricity of the spacecraft orbit



# Whole ballistic scheme of mission, accounting for sail surface degradation



Duration of spacecraft's movement to asteroid belt: 2116.08 days or approximately 5.8 years.

Total duration of launching spacecraft into working orbit is 6.8 years, considering passive motion before gravitational maneuver.

Trajectory of spacecraft with folded sail along intermediate heliocentric trajectory.

Transition to orbit in asteroid belt with epicenter of 3.6 AU and pericenter of 1.5 AU (purple dotted line).

Changes in trajectory due to soil degradation shown by orange dotted line.

## **Conclusion**

- Mathematical model of gravitational maneuver is constructed  
(acceleration, velocity, optical parameters, eccentricity, angles, aphelion parameters)
- Deployment of small solar sail in the asteroid belt, long mission
- Modern solar sail

# MAXWELL EQUATIONS, THEIR HAMILTONIAN AND BIQUATERNIONIC FORMS AND PROPERTIES OF THEIR SOLUTIONS

Classic system of Maxwell equations has the form: [Alexeyeva L.A.]

$$\begin{aligned} \operatorname{rot} E &= -\frac{\partial B}{\partial t}, \\ \operatorname{rot} H &= \frac{\partial D}{\partial t} + j^E(x, t), \end{aligned} \tag{1}$$

$$\begin{aligned} \operatorname{div} D &= \rho^E(x, t), \quad D = \varepsilon E, \\ \operatorname{div} H &= 0, \quad B = \mu H, \end{aligned} \tag{2}$$

$x \in R^3$ ,  $t \in R^1$ . Here electric conductivity  $\varepsilon$  and magnetic permeability  $\mu$  are constants in isotropic EM-medium. Vectors  $E, H$  are the tensions of electric and magnetic fields,  $B$  is magnetic induction,  $D$  is electric displacement,  $j^E(x, t)$  are the density of electric currents,  $\rho^E$  is the density of electric charges.

*Symmetric form of Maxwell equations:*

$$-\varepsilon \partial_t E + \text{rot} H = j^E(x, t), \quad \mu \partial_t H + \text{rot} E = j^H(x, t), \quad (3)$$

$$\varepsilon \text{div} E = \rho^E(x, t), \quad -\mu \text{div} H = \rho^H(x, t). \quad (4)$$

It's equivalent to MEqs when magnetic charges and currents are equal to zero:

$$\rho^H = 0, \quad j^H = 0. \quad (5)$$

The divergence from MEqs (3) gives *charges conservation law*:

$$\frac{\partial \rho^E}{\partial t} + \text{div} j^E = 0, \quad \frac{\partial \rho^H}{\partial t} + \text{div} j^H = 0. \quad (6)$$

## **Biquaternions**

We consider the functional space of biquaternions (Bqs.) in Hamilton's form of quaternions representation [13]:

$$\mathbb{B}(\mathbb{M}) = \{\mathbf{F} = f(\tau, x) + F(\tau, x)\}$$

on Minkowski space  $\mathbb{M} = \{(\tau, x) : x = \sum_{j=1}^3 x_j e_j\}$ ,  $f(\tau, x)$  is a complex functions,  $F(\tau, x)$  is a three-dimensional complex vector-function. They are locally integrable and differentiable on  $\mathbb{M}$  or, in general case, they are generalized functions [9];  $1, e_1, e_2, e_3$  are the basic elements in biquaternions algebra.

Summation and multiplication on  $\mathbb{B}(\mathbb{M})$  have the forms:

$$\mathbf{F} + \mathbf{B} = (f + F) + (b + B) \stackrel{\Delta}{=} (f + b) + (F + B),$$

# Biquaternionic and hamiltonian form of MEqs

If to introduce the biquaternions of  $EM$ -field:

*EM-tension*

$$\mathbf{A} = 0 + A = \sqrt{\varepsilon}E + i\sqrt{\mu}H$$

*charge-current*

$$\Theta = (i\rho + J) = i\rho^E / \sqrt{\varepsilon} + \sqrt{\mu}j^E,$$

*energy-impuls*

$$\Xi = 0,5 \mathbf{A}^* \circ \mathbf{A} = 0,5 (\bar{A}, A) - 0,5 [A, \bar{A}] = W + iP,$$

where

$$W = \frac{1}{2} \left( \varepsilon \|E\|^2 + \mu \|H\|^2 \right) \text{ is a density of energy of EM-field ,}$$

$$P = c^{-1} [E, H] \text{ is Pointing vector,}$$

then the Maxwell equations can be written in the form of the biwave equation:

*Biquaternionic form of Maxwell equations*

$$\nabla^+ \mathbf{A} = -\Theta \tag{16}$$

# Generalized solutions of MEqs biform

Solutions of MEqs biform are

$$\mathbf{A} = -\nabla^{-} (\psi * \Theta) + \mathbf{A}^0, \quad (20)$$

where spinor  $\mathbf{A}^0$  is arbitrary solution of homogeneous Maxwell equation:

$$\mathbf{A}^0 = \nabla^{-} \psi^0 + i \sum_{j=1}^3 \nabla^{-} (\psi^j e_j), \quad (21)$$

$$\square \psi^j = 0, \quad j = 0, 1, 2, 3, 4 \quad (22)$$

$$\psi^j = \int_{R^3} \varphi^j(\xi) \exp(-i(\xi, x) - i \|\xi\| t) d\xi_1 d\xi_2 d\xi_3, \quad \forall \varphi^j(\xi) \in L_1(R^3)$$

## LIGHT AS A PHOTONS CLOUD AND ITS BIQUATERNIONIC REPRESENTATION

Let consider the photons emitted by monochromatic charges-currents  $\Theta(x, \omega) \exp(-i\omega\tau)$ . They have the following biquaternionic representation through elementary photons by use biquaternionic convolution:

$$\Phi(x, \omega) = i\Theta(x, \omega) * \Phi_{\omega}(x) \quad (15)$$

For regular biquaternions this convolution has the next integral representation:

$$\Phi(x, \omega) = i \int_{R^3} \Theta(x - y, \omega) \circ \Phi_{\omega}^0(y, \omega) dy_1 dy_2 dy_3$$



**Example 2 (light sphere):**  $\Theta(x, \omega) = a\delta(b - \|x\|)$ . This is simple layer on sphere - singular generalized function. Photons cloud is described by next biquaternion:

$$\begin{aligned}
 \Phi(x, \omega) &= \phi(x, \omega) + \Phi(x, \omega) \\
 \Phi(x, \omega) &= -\frac{i}{4\pi} \delta(b-r) * \left\{ \frac{\omega e^{i\omega r}}{r} + \text{grad} \frac{e^{i\omega r}}{r} \right\} = \\
 &= -\frac{i}{4\pi} \left\{ \delta(b-r) * \frac{\omega e^{i\omega r}}{r} + \text{grad} \left( \frac{e^{i\omega r}}{r} * \delta(b-r) \right) \right\}, \\
 \phi(x, \omega) &= \frac{e^{i\omega r}}{2\omega r} \left\{ b \cos \omega b - i \left( r + \frac{1}{\omega} \right) \sin \omega b \right\}, \\
 \Phi(x, \omega) &= \frac{e^{i\omega r}}{2r} \left\{ \left( i - \frac{1}{\omega r} \right) \left[ \left( r + \frac{1}{\omega} \right) \sin \omega b + i b \cos \omega b \right] + \frac{\sin \omega b}{\omega} \right\} e_x
 \end{aligned} \tag{20}$$

**Example 3 (light ring):**  $\Theta(x, \omega) = a\delta\left(b - \sqrt{x_1^2 + x_2^2}\right)\delta(x_3)$ . This is simple layer on the ring in horizontal plane - singular generalized function. Photons cloud is described by next biquaternion:

$$\begin{aligned} \Phi(x, \omega) &= -\frac{i}{4\pi} H\left(b - \|x\|_2\right) \delta(x_3) * \left\{ \frac{\omega e^{i\omega r}}{r} + \text{grad} \frac{e^{i\omega r}}{r} \right\} = \\ &= -\frac{i\omega}{4\pi} H\left(b - \|x\|_2\right) *_{(x_1, x_2)} \frac{e^{i\omega r}}{r} + \frac{i}{4\pi} \left( e_{(x_1, x_2, 0)} \delta\left(b - \|x\|_2\right) *_{(x_1, x_2)} \frac{e^{i\omega r}}{r} \right) - \frac{ie_3}{4\pi} \frac{\partial}{\partial x_3} \left( H\left(b - \|x\|_2\right) *_{(x_1, x_2)} \frac{e^{i\omega r}}{r} \right), \end{aligned}$$

$$\phi(x, \omega) = -\frac{1}{2} \left( e^{i\omega \sqrt{\|x\|_2^2 + (x_3 - b)^2}} - e^{i\omega \|x\|} \right) + \frac{i\omega x_3}{2} \int_{\|x\|}^{\sqrt{\|x\|_2^2 + (x_3 - b)^2}} \frac{e^{i\omega \zeta}}{\sqrt{\zeta^2 - \|x\|_2^2}} d\zeta, \quad \|x\|_2 = \sqrt{x_1^2 + x_2^2},$$

$$\Phi(x, \omega) = \frac{i}{4\pi} e_{(x_1, x_2, 0)} \delta\left(b - \sqrt{x_1^2 + x_2^2}\right) *_{(x_1, x_2)} \frac{e^{i\omega r}}{r} - \frac{ie_3}{4\pi} \frac{\partial}{\partial x_3} \left( H\left(b - \|x\|_2\right) *_{(x_1, x_2)} \frac{e^{i\omega r}}{r} \right)$$

Here we use spherical coordinate system  $(r, \theta, \varphi)$  with vertical axis  $X_3$  and next designations:

$$\cos \theta = \frac{x_3}{\|x\|}, \quad \|x\|_2 = \sqrt{x_1^2 + x_2^2}, \quad y = (y_1, y_2, 0), \quad r(y) = \sqrt{y_1^2 + y_2^2},$$

תודה  
Dankie Gracias  
Спасибо شكراً  
Merci Takk  
Köszönjük Terima kasih  
Grazie Dziękujemy Dékojame  
Ďakujeme Vielen Dank Paldies  
Kiitos Täname teid 谢谢  
**Thank You** Tak  
感謝您 Obrigado Teşekkür Ederiz  
Σας Ευχαριστούμ 감사합니다  
Бондон  
Bedankt Děkujeme vám  
ありがとうございます  
Tack

**Bakhyt Alipova, Adjunct Professor**

**Department of Mechanical and Aerospace Engineering,  
University of Kentucky, Lexington, KY**

**Department of Mathematical and Computer Modeling  
International IT University,  
Almaty, Kazakhstan**



[alipova.bakhyt@gmail.com](mailto:alipova.bakhyt@gmail.com)